

SoftHandler: An Integrated Soft Robotic System for the Handling of Heterogeneous Objects

Franco Angelini^{1,2,3}, Cristiano Petrocelli², Manuel G. Catalano²,
Manolo Garabini^{1,3}, Giorgio Grioli² and Antonio Bicchi^{1,2,3}

Abstract—The picking performance of a robot can be severely affected by measurement errors, especially when handling objects that are fragile or irregular in shape and size. This is one of the main reasons why the problem of autonomously picking and placing objects is still open. In this work, we exploit the “embodied” intelligence of soft robotic technologies to propose an integrated system, named SoftHandler, capable of overcoming some of the limitations of traditional pick-and-place industrial robots. The SoftHandler integrates a novel parallel soft manipulator, the SoftDelta, and a novel soft end-effector, the Pisa/IIT SoftGripper. We describe the mechatronic design and control architectures of the system, including a learning technique able to preserve the natural compliance of the system. After that, we design a benchmarking method, and we experimentally compare the developed soft manipulator with its rigid counterpart. Experimental results with reference objects show that the proposed system has a larger grasping success rate than the rigid one and is subject to smaller interaction forces during the picking phase. Finally, we report an extensive experimental validation of the grasping capability of the SoftHandler with real objects in realistic, physically simulated, scenarios, as the ones of bin picking, grocery and raw food handling.

I. INTRODUCTION

Modern robotic technologies shine in picking and placing tasks where objects are orderly presented. However, rigid robots still provide unsatisfactory solutions when grasping and manipulating objects with a partially unknown geometry, or that are randomly placed in an unstructured environment. Traditional rigid robots may, indeed, drop or damage the manipulated objects and the possible occurrence of accidental impacts may also damage the robot itself. Inspired by biological systems, soft robots (both soft continuum [1] and soft articulated [2]) are system embedding compliant elements within their design. Such systems show an adaptive behavior, which is particularly useful when interacting with unknown objects [3] or unknown environments [4] and are robust to impacts [5]. In this work, we propose to exploit the properties of articulated soft robots to develop a device merging a soft manipulator and a soft end-effector that can be suitable in a set of scenarios characterized by imprecise knowledge of the position, shape and weight of movable objects and environment.

¹Centro di Ricerca “Enrico Piaggio”, Università di Pisa, Largo Lucio Lazzarino 1, 56126 Pisa, Italy

²Soft Robotics for Human Cooperation and Rehabilitation, Fondazione Istituto Italiano di Tecnologia, via Morego, 30, 16163 Genova, Italy

³Dipartimento di Ingegneria dell’Informazione, Università di Pisa, Largo Lucio Lazzarino 1, 56126 Pisa, Italy

frncangelini@gmail.com



Fig. 1. The SoftHandler: a soft articulated robotic system integrating a parallel delta manipulator, the SoftDelta, and a four fingers gripper, the Pisa/IIT SoftGripper.

Examples are bin picking, waste sorting and handling of groceries or raw food, in general. Being able to automate these processes is of particular importance since they involve several aspects that could be damaging for human beings. Indeed, they are highly repetitive tasks that may force operators to work in hazardous environments like refrigerated cells or in contact with sharp or unhealthy items.

Looking at these common logistic tasks, and how humans perform them, top-down grasping approaches are usually favored for several reasons that include also the typical layout of factory lines. During top-down grasps human beings tend to completely envelop with the fingers the object to be grasped [6], [7]. This movement is commonly known as caging primitive, and it is the same performed also by many conventional robotic solutions. It is also worth mentioning that human beings, during the top-down approaching phase,

tend to have many interactions with the environment, e.g. with the planar surface where the object is placed, in order to realize better grasps, as fruitfully highlighted in [6], [7].

Inspired by these observations, in this paper we propose an integrated system, named SoftHandler, capable of overcoming some of the limitations of traditional pick-and-place industrial robots, also in presence of limited vision information. Furthermore, we discuss and present the control architecture that underpin such integration, showing and benchmarking its performance in both simulated and realistic scenarios.

For the manipulator, we adopt a parallel delta kinematics [8]. The delta configuration is already very common in industry, ensuring fast and precise motions. The design of the robot will be based on Variable Stiffness Actuators (VSAs) [9]. VSA technology allows either a soft behavior, when robustness and adaptivity are preferred, or a rigid behavior, when accuracy and precision are needed. In [10], the authors employed an early proof-of-concept of a VSA delta robot as an experimental platform to validate a specific control algorithm. However, no description of its design nor validation of its performance were reported. Moreover, this prototype had a small size and a very limited payload and was not equipped with any end-effector. In this work, we leverage on this past experience to propose a novel VSA delta robot, the SoftDelta, with larger workspace, higher dynamic performance and higher payload, opening, as a consequence, the possibility to integrate the system with a suitable robotic end-effector.

In [4], [11] it is shown that soft end-effectors can exceed the limits of traditional rigid grasping systems. Their carefully designed mechanical transmissions for safe interaction, high resilience and intrinsic adaptivity, yield gentle but firm grasp of objects with very different shape, even when the environment is partially constrained or not completely known. Literature proposes a wide range of soft end-effectors ranging from continuously deformable grippers ([12], [3], [13]) up to articulated soft systems ([14], [15], [16]). The end-effector presented in this paper is an articulated soft gripper inspired by the Pisa/IIT SoftHand [2] technology. This device has a simple design, which is particularly suited for top-down pick-and-place tasks performed e.g. with a delta manipulator. Furthermore, the gripper preserves a low level of control complexity thanks to the presence of only one motor, and a high level of robustness. It is worth noting that a device with similar appearance as the SoftGripper but different design, was shown in [17]. In that paper, mostly devoted to describing the waterproofing of underwater grasping devices, the gripper was not the subject of any detailed description or analysis. Indeed, the actuation solution, the field of use and the planning approach were completely different, and problems discussed in this paper have not been addressed previously.

In this work, we present the SoftHandler, a device for heterogeneous pick and place tasks that integrates a novel parallel soft manipulator, the SoftDelta, and a novel soft end-effector, the Pisa/IIT SoftGripper. In addition to the

mechatronic characteristics of the SoftHandler components, we provide a theoretical analysis of the Cartesian stiffness of the manipulator and we describe and validate the control architecture of the entire system, showing also how learning control techniques can preserve its natural compliant behavior. Then, we compare the manipulator with its rigid counterpart, showing how the proposed solution can be exploited in order to obtain better performance in terms of grasped objects, merged to reduced effects of impact forces on the items and on the robot actuation structure. This is one of the few cases in literature which presents a direct juxtaposition of an articulated soft robot with a comparable traditional rigid robot, and that analyzes and discusses their performance. Finally, to validate the system, we test the SoftHandler (combined with a minimalistic vision system), in realistic use case scenarios, including bin picking, grocery and raw food handling. Obtained results show promising performance, in terms of grasping success rate, versatility and object integrity.

The paper is organized as follows: in Sec. II we discuss about issues related to traditional rigid robots, taking some examples of industrial scenarios. In Sec. III we describe the design and the control methodologies of the developed device. In Sec. IV we characterize the proposed system, and we benchmark its grasping performance in comparison with its rigid counterpart. In Sec. V we show how the SoftHandler performs in realistic, physically simulated, scenarios, and we discuss results. In Sec. VI we discuss about the performance and failures of the proposed system. Finally, in Sec. VII we draw the conclusions.

II. THE CHALLENGE

In order to define the outlines of the problem, we start by reviewing some relevant examples of unsolved industrial pick-and-place tasks, and we discuss the main challenges to be addressed.

In *bin picking* (Fig. 2(a)) objects are homogeneous but often present complex geometrical shapes and are placed with random orientations. Furthermore, the presence of bin walls and other fixtures may hinder robot motion or cause undesired collisions. In *grocery handling for packaging* (Fig. 2(b)), a very common example in the recent practice of dark storing, the goods are well organized, but they come in a wide variety of shapes, textures, weights and sizes, they are often delicate and can be easily damaged by improper manipulation. In *raw food handling* after harvesting (Fig. 2(c)), as in grocery handling, the shape, weight, size, orientation and stiffness of the objects differ extensively. Furthermore, raw food is usually placed into crates without any particular organization. Finally, *waste sorting* (Fig. 2(d)) is an example where irregularity and randomness of the objects are extreme, as are the physical properties (density, weight, shape, stiffness etc.) of items such as cardboard, packaging materials, glass fragments, hard pieces of scrap metal or wood.

All these cases share the possible issue of inaccuracy in the detection of the object pose. This may cause a grasp to

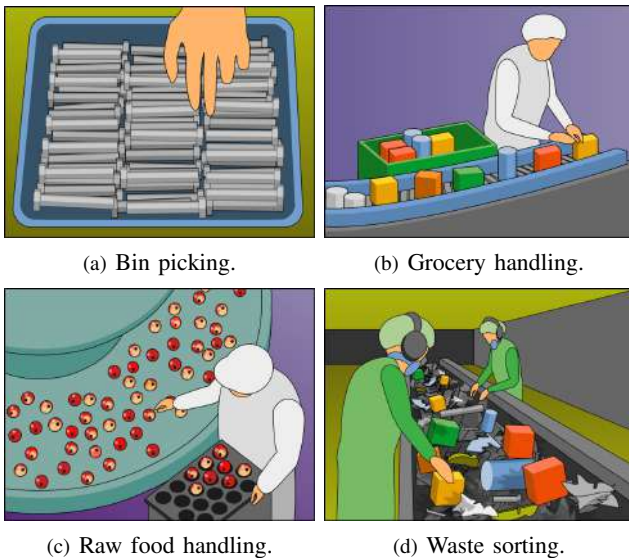


Fig. 2. Examples of industrial pick-and-place tasks that can benefit from the use of soft robots. Handling heterogeneous, unordered or fragile objects is a challenge yet hard to be accomplished by traditional rigid robots.

fail, or in some cases, can generate large interaction forces that can damage the robot or the object. It is relevant to highlight how these different contexts of use can present several possibilities in terms of object placement. Sometimes, also in the same context, objects can be placed randomly or in a fixed and predefined configuration. This is the case, for example, of food handling in dark stores. In this scenario, objects can be disposed in bins randomly (as e.g. courgettes or bananas) or with specific grids (as e.g. apples or peaches). Such variability is one of the leading factors for the need of versatile handling systems.

In recent years, these tasks are getting more and more attention by the robotic community. Soft Robotics Inc.¹ develops soft grippers for bin picking and raw food handling, while Ocado² proposes solutions for raw food and grocery handling. Amazon Robotics³ sets challenges for improving technologies for grocery handling. ZenRobotics Ltd.⁴ designs waste sorting systems. Pick-it N.V.⁵ develops vision system for bin picking tasks.

In this work, although we present results also in the field of grocery handling and bin picking, we will especially focus on raw food handling, applying the proposed system, mostly, to this scenario. In the state of the art there are several investigations related to this topic [18], [19], [20]. In [20] a robotic system for the manipulation of onions and artichokes is presented, the robot consists of a rigid delta robot with a vacuum suction cup. The differences with our solution are that our manipulator has flexible joints, thus is able to exert

lower interaction forces. Furthermore, the end-effector they employ is specifically designed for onions and artichokes, while our solution can be applied to several different objects and does not rely on suction systems, thus it does not require pressured air to function.

It is worth noting that, historically, suction grippers have been broadly used in the contexts discussed in this paper, anyway, such systems present limits when grasping porous objects as fresh fruit and vegetables, or objects with slippery surfaces, as the ones that can be present in waste sorting scenarios (i.e. presence of humidity or dust) or bin picking (i.e. presence of oils or moistures). Moreover, often, suction grippers need different design or control strategy depending on the item-to-be-grasped.

In order to grasp heterogeneous objects and develop versatile systems, it is authors' opinion, that an adaptive fingered gripper is preferable to end-effectors based on suction technologies.

III. SOFTHANDLER DESIGN

The SoftHandler is obtained by the combination of a novel soft articulated end-effector, the Pisa/IIT SoftGripper, and of a novel parallel manipulator equipped with soft actuators, the SoftDelta. The entire system is then mounted on a $1 \times 1 \times 1$ m rigid structure. In the following, we describe the design of each component, and we present and discuss the control architecture and the different control algorithms that can be employed on the system, considering also the different circumstances and scenarios of use.

A. Pisa/IIT SoftGripper

Simplicity (i.e. under-actuation), robustness and adaptivity (i.e. softness and compliance) are the main features that led to the development of the Pisa/IIT SoftHand [2]. The same driving ideas underlie the design of the Pisa/IIT SoftGripper (Fig 3(a)): the 12 DoFs (Degrees of Freedom) which make up this device are driven by only 1 DoA (Degree of Actuation), while the embedded elastic elements guarantee a behavior compliant to the environment and robust to external forces.

Although the SoftGripper shares some of the basic components of the Pisa/IIT SoftHand (e.g. compliance through underactuation), it is completely different in most respects, including the kinematics, number and length of the fingers. While the SoftHand was designed for reproducing the first synergy observed in human grasps and has an architecture particularly suited for versatile grasping, the SoftGripper is inspired to the caging primitive [6], [7], i.e. a grasping approach where the object is fully enveloped by the fingers. Furthermore, the different kinematics and longer fingers of the SoftGripper allow to grasp larger objects.

The Pisa/IIT SoftGripper is composed of four fingers placed in a cross configuration, exhibiting an axial symmetry. The employed fingers are a derivation of the ones used in the Pisa/IIT SoftHand ([2]). Each of them is composed of a series of four modular phalanges connected through a revised compliant version of the Hillberry rolling joint that enables a soft and safe behavior, and allows to recover

¹<https://www.softroboticsinc.com/>

²<https://www.ocadotechnology.com/>

³<https://www.amazonrobotics.com/>

⁴<https://zenrobotics.com/>

⁵<https://www.pickit3d.com/>

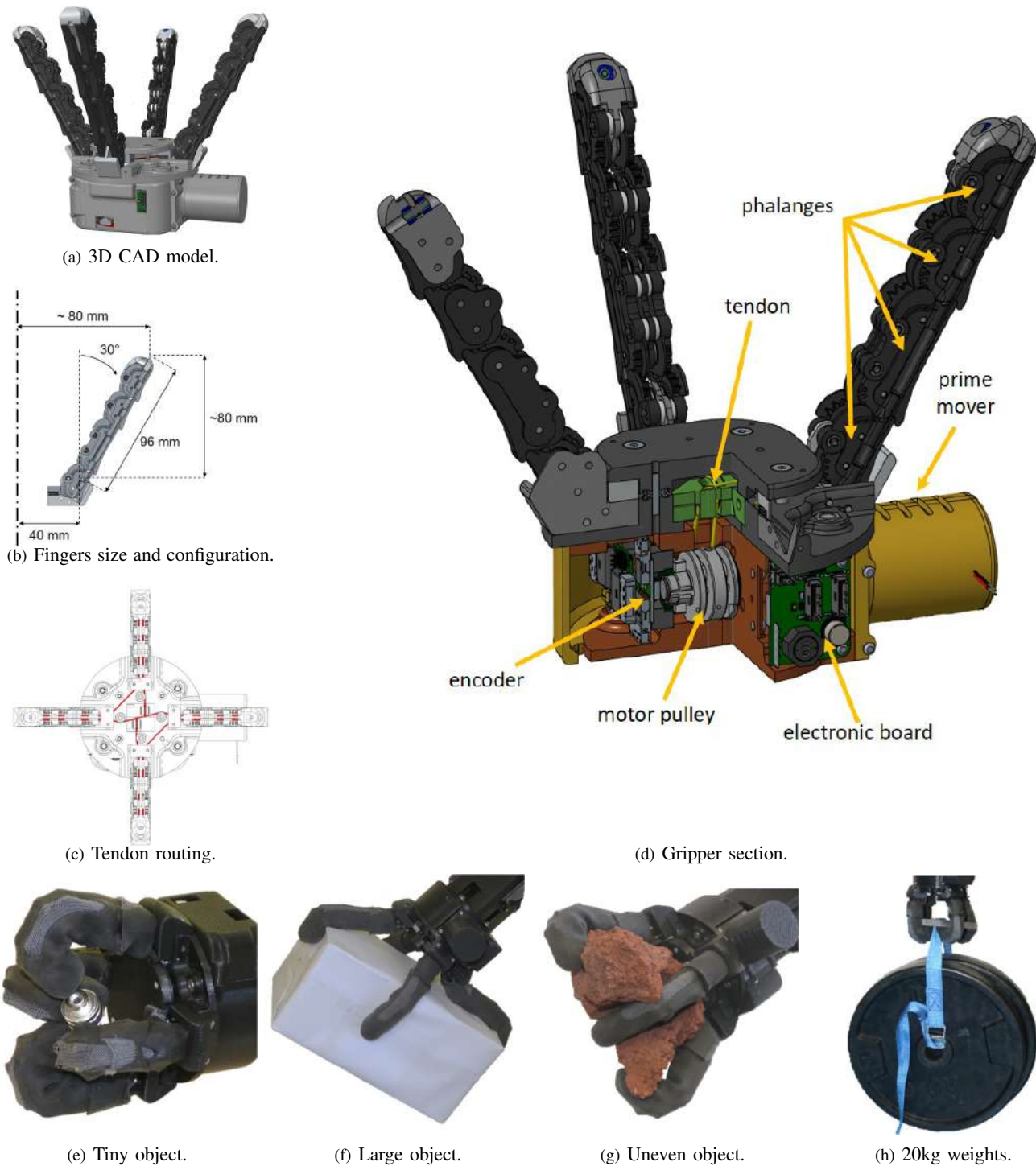
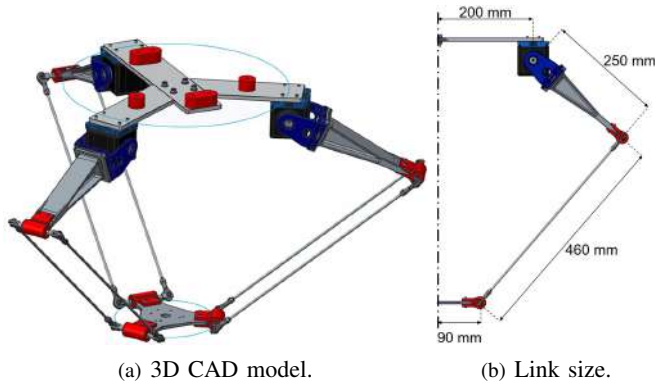


Fig. 3. (a) 3D CAD model of the SoftGripper. (b) Fingers design and configuration. The fingers size and orientation permits to grasp heterogeneous objects. (c) The tendon routing of the differential mechanism ensures a synchronized closure of the fingers. (d) Three-dimensional section of the CAD model. In the figure are highlighted the phalanges, the prime mover, the electronic board, the encoder, the motor pulley and the tendon. (e) SoftGripper grasping a tiny reel ($\varnothing 20 \times 20$ mm). (f) SoftGripper grasping a large box ($210 \times 115 \times 110$ mm): the design of the fingers enables the dis-articulation of the phalanges that permits to grasp objects larger than the gripper envelope volume. (g) Softgripper grasping a rock with uneven surface and geometry. (h) SoftGripper lifting 20kg.

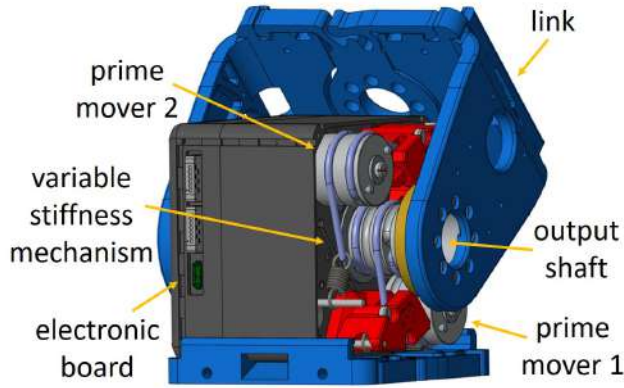
from fingers overextension. The SoftGripper has proximal phalanges longer than the SoftHand, increasing the size span

of the graspable objects. Fig. 3(b) shows the size and the orientation of the fingers. Each finger is 96mm long and



(a) 3D CAD model.

(b) Link size.



(c) qbMove Advanced 3D CAD model.

Nominal torque	Nominal speed	Stiffness Range	Rotation range	Weight
5.5Nm	5.5rad/s	[0.5, 83.5]Nm/rad	$[-\pi, \pi]$ rad	0.45kg

(d) Main features of qbMove Advanced actuator.

Fig. 4. Characteristics of the SoftDelta. (a) SoftDelta 3D CAD model. (b) Link size and orientation. (c) Details of the actuator. The agonist-antagonistic mechanism basing the variable stiffness structure is clearly visible in figure, while the prime movers and the electronic board are covered by the external frame (black color). (d) Nominal characteristics of the variable stiffness actuation mechanism.

leans 30deg outside the vertical to the palm. The palm of the gripper has a diameter of 80mm leading to a distance of ~ 160 mm between the tip of two opposite fingers when the gripper is fully open. This design produces a grasping volume that equals an 80mm diameter sphere.

The actuation of the gripper is carried out through a differential transmission based on a tendon-pulley mechanism. A single Dyneema tendon distributes the motion of the prime mover to all 12 joints. The careful regulation of the elastic elements and of the tendon routing (Fig. 3(c)) ensures a synchronized closure of all the fingers. The actuator is a 15Watt Maxon motor DCX22S with a GPX22 gearhead (reduction ratio 83 : 1), equipped with two 12 bit magnetic encoder (Austrian Microsystems AS5045). The actuator, together with the embedded electronic board ([2]), are placed under the gripper palm (Fig. 3(d)). Fig. 3(d)

highlights the main components of the device, in particular how the tendon is connected to the prime mover through a pulley. The total weight of the gripper is 590g.

The SoftGripper is equipped with an off-the-shelf glove with padded rubber surfaces in such a way to increase contact grip and compliance. Furthermore, thanks to the glove, all the grooves and openings on the fingers are covered, achieving one of the main requirement for food grippers: hygienic performance [18]. Indeed, the glove avoids collecting moisture and small particles of food material and, since it is removable, it is also easy to wash and clean.

Finally, it is worth noting that food handling tasks may involve also the presence of water or humidity. Since fingers of the Pisa/IIT SoftGripper do not incorporate any sensor or electronics, they are able to work well also in wet environments, indeed control and power electronic boards are protected and covered by the gripper frame. Fig. 3(e-h) show the SoftGripper grasping various objects with different size, shapes and weights. Thanks to the compliant design of the fingers, the proposed device is able to grasp small objects and objects larger than the designed gripper workspace. Fig. 3(e) shows the developed device picking a tiny reel ($\varnothing 20 \times 20$ mm), while Fig. 3(f) shows the gripper grasping a large box ($210 \times 115 \times 110$ mm), larger than the gripper envelope volume. Fig. 3(g) depicts the gripper grasping a rock with uneven surface and geometry. Finally, Fig. 3(h) shows the SoftGripper lifting a 20kg weight. More examples are reported in the attached video footage.

B. SoftDelta

The SoftGripper alone is not enough to guarantee a damage-free manipulation as the robot mounting the gripper can also be responsible for large interaction forces. Focusing on adaptability and robustness, we developed a parallel soft manipulator. The idea is to employ a parallel architecture to reduce the ratio between the mass of the robot and the mass of the payload. On the other hand, the compliance of the joints works as a low-pass filter for interaction forces between the robot and the object to be grasped. Thus, it allows to preserve the object integrity and to increase the robot adaptability, hence enhancing the grasping capability.

The SoftDelta is composed of three VSA-powered kinematic chains that connect the base of the robot to the common end-effector (Fig. 4(a)). The three legs are identical and present a series of three joints, i.e. one revolute and two universal joints. The revolute joint is attached to the fixed base and is the only active joint. The second link of each kinematic chain has a parallelogram structure that allows the implementation of the two universal passive joints. Indeed, each universal joint is composed of three non-collocated revolute joints. Fig. 4(b) reports the size of the SoftDelta kinematic chains. Notoriously, the closure of the kinematic chains of the delta robot limits the end-effector movements to pure translation in the XYZ directions, making this kind of robot particularly suited for top-down grasping tasks.

The adopted VSA units are the *qbmoves Advanced* (Fig. 4(c)), a derivation of the *VSA-CubeBot* [2]. These are mod-

ular actuators with limited power (15Watt), mainly intended for research purposes. Fig. 4(d) reports the main features of these devices. The qbmove Advanced implements an agonistic-antagonistic mechanism (Fig. 4(c)): the output shaft of each actuator is connected through a non-linear elastic transmission to two motors. Moving the motors in opposite directions leads to a variation of the compliant behavior of the robot. Each qbmove Advanced is equipped with a custom electronic board [2] which implements the low-level control (PID) of the motors. The same board is used to connect in series multiple qbmove units with a daisy-chain topology. The position of each motor and of the output shaft is measured with a AS5045 magnetic encoder, with a resolution of 12 bit.

The spring characteristic of the actuator is

$$\begin{aligned}\tau &= k_1 \sinh(a_1(q - \theta_1)) + k_2 \sinh(a_2(q - \theta_2)) \\ \sigma &= a_1 k_1 \cosh(a_1(q - \theta_1)) + a_2 k_2 \cosh(a_2(q - \theta_2)),\end{aligned}\quad (1)$$

where $\tau \in \mathbb{R}$ is the elastic torque, $\sigma \in \mathbb{R}$ is the joint stiffness, $q \in \mathbb{R}$ is the link position, and $\theta_1 \in \mathbb{R}$ and $\theta_2 \in \mathbb{R}$ are the positions of the two motors embedded in the VSA. The model parameters⁶ are $k_1 = 2.6\text{Nmm}$, $a_1 = 9\text{rad}^{-1}$, $k_2 = 1.1\text{Nmm}$ and $a_2 = 9\text{rad}^{-1}$.

The 0rad reference position of each actuator is the one depicted in Fig. 4(b), i.e. an angle of $\frac{\pi}{4}\text{rad}$ between the base of the robot and the actuator link. A positive turning angle of the actuator leads to a lifting of the link.

Given (2), it is possible to define the joint stiffness matrix $K_J \in \mathbb{R}^{3 \times 3}$ as

$$K_J = \begin{bmatrix} \sigma_1 & 0 & 0 \\ 0 & \sigma_2 & 0 \\ 0 & 0 & \sigma_3 \end{bmatrix}, \quad (3)$$

where $\sigma_i \in \mathbb{R}$ is the stiffness of the i -th actuated joint. Varying the stiffness of the joint through (2) allows to shape the Cartesian stiffness of the manipulator. In particular, the Cartesian stiffness $K_C \in \mathbb{R}^{3 \times 3}$ is defined as [21]

$$K_C = -\frac{\partial \mathbf{w}_e}{\partial \mathbf{x}} = -\frac{\partial J^{-T} \boldsymbol{\tau}}{\partial \mathbf{x}} = J^{-T} K_J J^{-1} - \frac{\partial J^{-T}}{\partial \mathbf{x}} \boldsymbol{\tau}, \quad (4)$$

where $\mathbf{w}_e \in \mathbb{R}^3$ is the wrench applied at the end-effector, $\mathbf{x} \in \mathbb{R}^3$ is the Cartesian displacement, $\mathbf{q} \in \mathbb{R}^3$ is the vector of the joint positions, and $\boldsymbol{\tau} \in \mathbb{R}^3$ is the vector of the actuation torque. $J(\mathbf{q}) = \partial \mathbf{w}_e / \partial \mathbf{q} \in \mathbb{R}^{3 \times 3}$ is the Jacobian matrix of the manipulator. This can be evaluated differentiating the kinematics of the system. The direct kinematics, computed through the three spheres intersection algorithm, and the inverse kinematics, geometrically evaluated, are reported in [22]. Eq. (4) can be used to estimate the interaction forces due to a displacement of the end-effector caused by the environment.

C. Control Description

From a control point of view, literature proposes a wide range of techniques to control articulated soft robots. Examples are [23] where the authors employ a backstepping

based algorithm, or [24] where a feedback linearization based technique is presented.

The major drawback of all these methods is that they are strongly model-based, thus they require an accurate knowledge of the system, which is usually hard to obtain in soft robots. Moreover, model-based feedback techniques usually replace the system physical dynamics with a desired one, nullifying the advantages obtained by embedding physical compliance in the robot. This phenomenon is even more pronounced in model-free high-gain feedback methods, which have the drawback of increasing the joint stiffness hindering the mechanical impedance of the system [10].

A solution to all these issues is employing a feedforward learning technique. Indeed, the learning process allows to improve the tracking performance despite the inaccuracy of the robot model, while the feedforward architecture allows the desired compliance preservation. Among all the possible frameworks, Iterative Learning Control (ILC) allows to increase the tracking performance through the repetition of the task, exploiting the experience accumulated during past trials.

In [10] a feedforward control method based on an ILC approach is presented. This solution merges a low-gain feedback component and an iteratively refined feedforward term. Given a desired joint reference $\hat{\mathbf{q}} \in \mathbb{R}^3$, this technique leads to a position control action $\mathbf{u} \in \mathbb{R}^3$ able to simultaneously maintain the natural behavior of the system, while achieving satisfying tracking performance with limited knowledge of the robot model. The controller has a decentralized architecture, and the control law applied to the i -th joint is

$$u_i^t = u_i^{t-1} + K_{\text{up},i} e_i^{t-1} + K_{\text{fb},i} e_i^t, \quad \forall i = 1 \dots 3, \quad (5)$$

where $u_i \in \mathbb{R}$ is the control input of the i -th joint, $e_i = [\hat{q}_i, \dot{\hat{q}}_i]^T - [q_i, \dot{q}_i]^T \in \mathbb{R}^2$ is the i -th joint tracking error signal, and $K_{\text{up},i} \in \mathbb{R}^{1 \times 2}$ and $K_{\text{fb},i} \in \mathbb{R}^{1 \times 2}$ are the i -th joint update and feedback gain matrices respectively. t is the iteration index, thus e_i^t is the error signal at the current iteration (i.e. feedback), while e_i^{t-1} is the error signal at the previous iteration.

The feedforward term at the first iteration u_i^0 is chosen based on an approximation of the robot dynamics. We consider each joint as decoupled, and we identify the dynamic parameters through a step response approach. Despite the rough estimation of the robot model, the learning phase allows to achieve good tracking performance. Indeed, the convergence of the iterative method is guaranteed thanks to a proper setting of the gain matrices $K_{\text{up},i}$ and $K_{\text{fb},i}$. Finally, $K_{\text{fb},i}$ is designed through a Linear Quadratic Regulator (LQR) method. Since the resulting feedback component $K_{\text{fb},i} e_i^t$ is small, the robot compliance results substantially unaltered. Please refer to [10] for more details about the control algorithm.

The major drawback of an ILC-based technique is that each desired trajectory requires a distinct learning process. This means that, if the task requires to move freely inside the device workspace, each possible motion with each possible payloads should be learned beforehand. This solution is so

⁶<https://qbrobotics.com/wp-content/uploads/2016/03/qbmove-Advanced-datasheet.pdf>

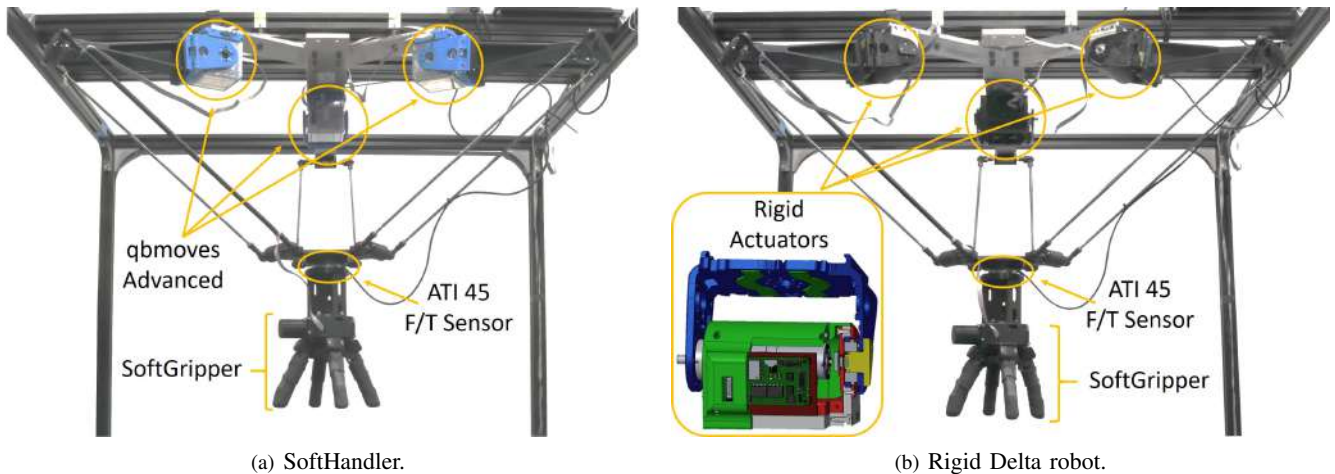


Fig. 5. Experimental devices: (a) SoftHandler (b) Rigid Delta. Both devices have equal size and are equipped with a SoftGripper and an ATI mini 45 force/torque sensor. In the detail of (b) is depicted the actuator of the Rigid Delta robot. The electronic board, the prime mover and the encoder are clearly visible in the figure .

time-consuming to be often impracticable, thus generalization method should be adopted. Future works will focus on the generalization of the learned control action w.r.t. the desired trajectory.

For these reason, for the tasks not involving fixed end-effector trajectories we adopt a feedforward approach based on the inverse kinematics of the robot. This is flanked by a low tuned PID controller to increase the tracking performance. This approach presents lower tracking performance and an alteration of the system joint stiffness proportional to the feedback proportional gains.

IV. SYSTEM CHARACTERIZATION

In this section we characterize the SoftHandler system, in terms of grasping performance and forces exchanged with the object and the environment. To this end, we establish a benchmarking method, and we build a rigid system with comparable kinematics and actuation power. Furthermore, forces obtained at the end-effector are compared to the ones estimated by the Cartesian stiffness model.

A. Grasping Performance

To establish a baseline for the evaluation of the SoftHandler performance we developed a benchmark task, and we did a comparison with an equivalent rigid manipulator based on the same architecture of the SofDelta but actuated by rigid motors. We specifically designed the benchmarking manipulator in order to have two systems with equal kinematic structures and analogous actuation performance, i.e. the motors have the same power of the ones used in the SoftDelta. Indeed, as highlighted by (4), different kinematics would lead to different mapping of the joint stiffness into Cartesian stiffness, biasing the analysis. In this experiment both manipulators are intentionally equipped with the same soft end-effector, i.e. the Pisa/IIT SoftGripper. The reason behind this choice is twofold. First, the goal of the proposed device is to be able to handle fragile and heterogeneous

objects without damaging them. Thus, a rigid gripper would not be able to satisfy the fragile object requirement. Indeed, it is well known in the literature that soft end-effectors shows better performance in grasping fragile and uneven objects [4], [11]. The second reason for the choice of the same end-effector is to highlight the differences due to the actuation mechanism rather than on the overall device.

1) *The Benchmark:* The performed task is grasping spherical objects with different size and weight. The goal of this benchmark is to compare the performance of the SoftHandler (Fig. 5(a)) with the performance of a rigid manipulator in terms of grasping acquisition region [11] and applied contact forces when an undesired displacement between the robot end-effector and the object to-be-grasped occurs. This issue may arise in several scenarios, e.g. when there are trajectory tracking errors or measurement inaccuracies due to the vision system. In order to objectively test the performance in presence of a displacement between the end-effector and the object, we try to grasp the same object without any vision system support, tracking the same trajectory but varying the object position.

After each trial, the object is moved in the XY plane, changing the displacement from the end-effector. This procedure is performed employing a plate with holes as reference frame (sketched in Fig. 6(a)): each hole fixes the position of the object thanks to an object-stand equipped with a dowel pin (Fig. 6(b)). The pin fixes the stand to the plate, ensuring a precise positioning of the object, but it does not constrain the object, leaving it free to be moved by the robot during the interaction. The holes on the plate are organized as a 9×9 mesh grid with nodal distance 10mm (Fig. 6(a)). This translates into 81 possible different positions in the XY plane for the object and a maximum displacement of ~ 57 mm.

The plate is placed on the frame under the device in a way that the center of the grid is aligned with the Delta Robot base center, i.e. the intersection of the normals to the rotational axis of the three joints. In Fig. 6(a) is depicted a

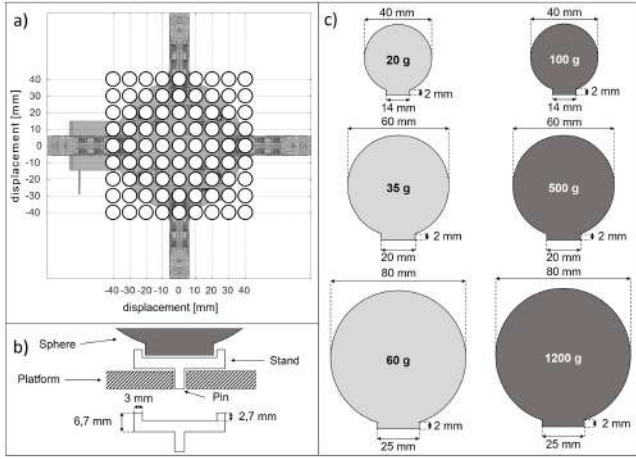


Fig. 6. Sketch and sizes of the experimental setup. (a) Sketch of the mesh grid employed as reference position for the objects. In the sketch is depicted also the SoftGripper in order to show the relative position between the grid and the end-effector. (b) Sketch of the object-stand used to ensure that the object position is accurate at the beginning of the grasping task. Note that the stand leaves the object free to be moved due the interactions with the robot end-effector. (c) List of the objects to be grasped: six spheres spanning from 40mm diameter and 20g weight to 80mm diameter and 1200g weight.

sketch of the grid-gripper relative position. It is worth noting that the SoftGripper fingers are aligned with the grid lines.

We performed this experiment with both the SoftDelta and the rigid delta manipulator (Fig. 5(b)), using six different spherical objects with different sizes and weights. In Fig. 6(b,c) are reported the dimensions of the pinned object stand and of the objects.

2) *Experimental Setup*: We built the parallel Rigid Delta manipulator (Fig. 5(b)) sharing equal size and workspace with the proposed compliant device and differing only in the actuators. The SoftDelta is actuated by three qbmoves Advanced (Fig. 4(c)), while the Rigid Delta is actuated by three Maxon motor DCX22S with a GPX22HP gearhead (reduction ratio 231 : 1), equipped with the AS5045 magnetic encoder and the electronic board described in [2] (detail in Fig. 5(b)). As for the qbmoves, the electronic board manages sensing, communication and low-level control (PID). Fig. 5 compares the two devices, showing their main components. It is worth noting that both devices are equipped with the Pisa/IIT SoftGripper.

A force sensor (6-axis force/torque ATI mini 45) is placed between the gripper and the delta mobile platform (Fig. 5) to measure the interaction forces applied during the contact. The weight of the sensor is 91.7g.

3) *Experimental Procedure*: In each trial the parallel manipulator starts with the end-effector lifted over the plate, and the gripper is set to a pre-closure configuration to avoid singularities of the fingers. Then, the end-effector moves vertically until the fingertips are nearly touching the plate. At this point, the gripper closes and tries to grasp the object.

Independently from the object weight, size and position the grasping approach is the same and is pre-tuned on the big sphere size. After the grasping phase, the robot lifts the end-effector. To summarize, the joint reference is a minimum jerk trajectory from 0.7854rad to -0.2443 rad in 1.5s and an opposite trajectory to return to the starting position.

As one of the performance indexes, we chose to use the norm of the force measured by the sensor. The mesh grid on the plate is spanned with all spheres and both devices. The goal is to analyze the performance of the robots in presence of a variation in the object size and weight and an error in the relative position between the object and the end-effector.

In this experiment the mechanical behavior of the SoftDelta is set to soft (i.e. $\theta_{1,i} - \theta_{2,i} = 0$ rad, $i = 1, \dots, 3$) to enhance adaptability. In order to preserve the robot compliance, the adopted control strategy is the one proposed in [10] and briefly presented in section III-C, i.e. a feedforward control method based on an ILC approach.

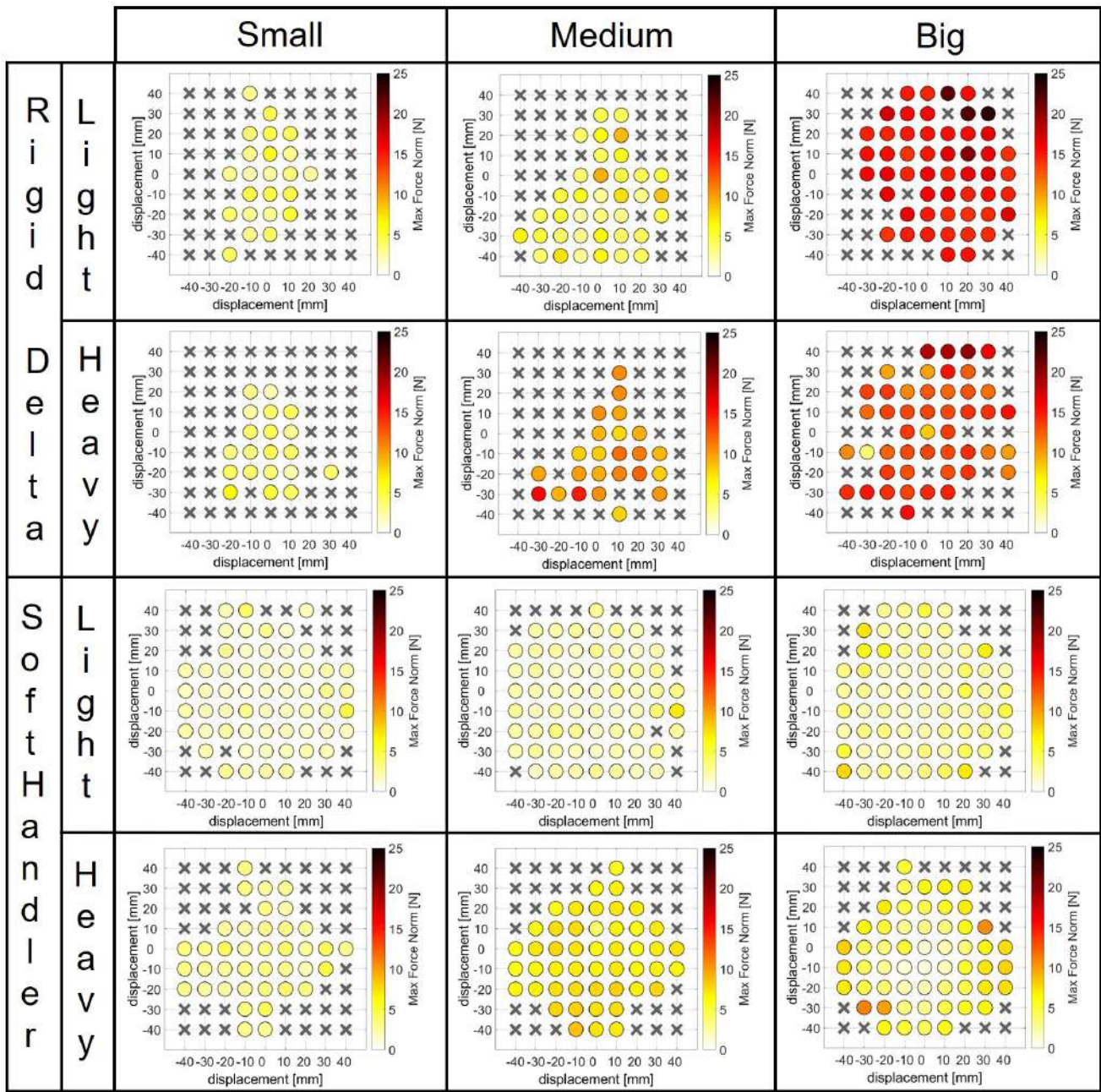
4) *Results*: The experimental results are reported in Fig. 7. Each map represents the grasping results for a given robot and a given sphere: a cross marker means that the robot failed to grasp the object given that displacement, while a circle represents a success. The color-map of the circles represents the maximum norm of the forces applied by the robot during the contact and grasping phase: darker colors translates into larger forces. For each case the table reports: the success percentage, the mean value and the standard deviation of the maximum norm of the applied forces and the value of the maximum norm.

Fig. 8 summarizes the successful grasp percentage in function of the maximum displacement for each robot and each sphere. Each value on the x -axis represents the radius of a circle centered in the center of the grid. The corresponding values on the y -axis represent the successful grasp percentage for each sphere when the object to-be-grasped is placed within that circle. In order to better analyze the results, in Fig. 8 are reported also the results averaged over the size and weight of the spheres.

Finally, Fig. 9 compares the grasping sequence of the big heavy sphere placed in the grid position $[30, -30]$ mm for the Rigid Delta and the SoftDelta respectively.

5) *Discussion*: Independently from the size and the weight of the considered object, the SoftHandler presents a higher grasping success rate than the Rigid Delta robot (Fig. 7). Indeed, the average of the success rate between all spheres and all displacements (Fig. 8(l)) is 68% for the SoftHandler, while it is 41.8% for the Rigid Delta. Furthermore, it is worth noting that, in the soft robot case, the success area does not present any hole relatively to the center of the grid, on the contrary of the rigid robot case. The better performance of the SoftHandler can be attributed to one of the main features of soft robotic technologies, i.e. the adaptivity to the environment.

Fig. 8 shows that the proposed device presents a higher grasping success rate for each sphere and each maximum displacement. Fig. 8 shows also that, for both manipulators, the grasping performance worsen when the maximum dis-



		Small				Medium				Big			
		% Success	Mean [N]	Std [N]	Max [N]	% Success	Mean [N]	Std [N]	Max [N]	% Success	Mean [N]	Std [N]	Max [N]
Rigid	Light	28,4	3,51	0,97	5,34	45,7	4,78	1,77	9,12	64,2	15,62	2	23,29
	Heavy	24,7	3,56	1	6,34	29,6	10,03	1,99	15,58	58	13	2,61	19,51
Soft	Light	71,6	1,88	0,58	4,63	79	2,16	0,77	6,92	82,7	3,11	1,39	7,66
	Heavy	48,2	2,92	0,57	4,57	59,3	6,82	0,78	8,57	67,9	5,05	2,29	10,82

Fig. 7. Comparison between the SoftHandler and the Rigid Delta Robot in terms of grasping capability and applied contact forces when there is a displacement between the end-effector and the object. In the figure each map represents the grasping results for a given robot and a given object: a cross marker means that the robot failed to grasp the object in that position, while a circle represents a success. The colormap of the circles represents the maximum norm of the applied forces during the contact and grasping phase: darker colors represents larger forces. In the table are reported for each case: the success percentage, the mean value and the standard deviation of the maximum norm of the applied forces and the value of the maximum norm.

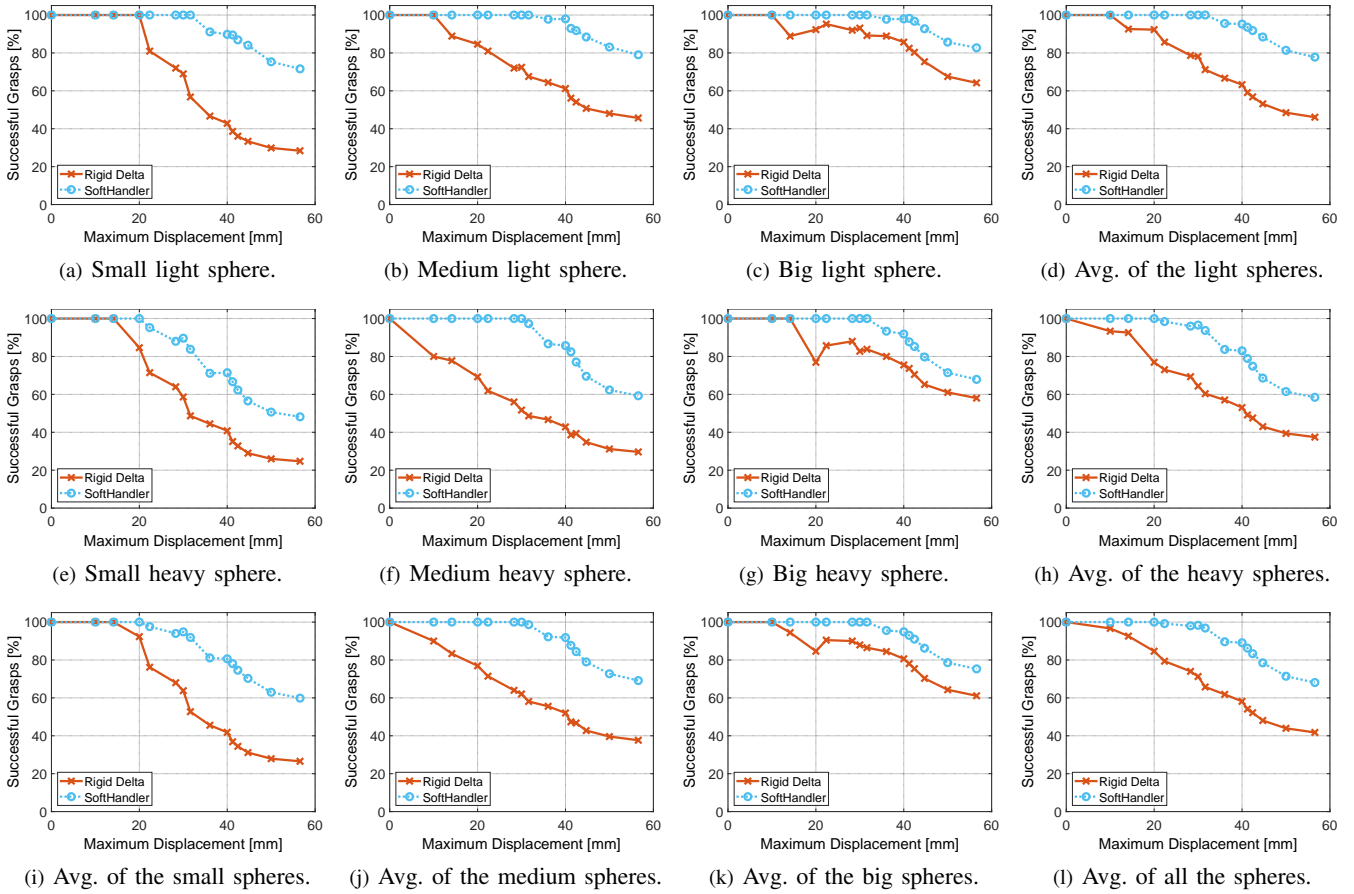
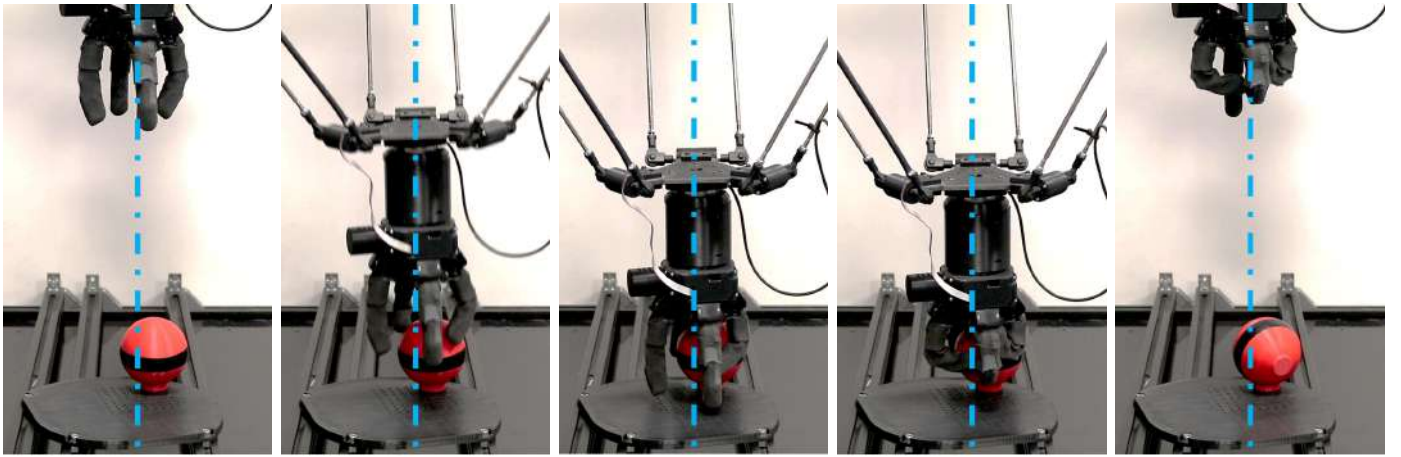


Fig. 8. Successful grasp percentage based on the maximum displacement between the end-effector and the object. Each value on the x -axis represents the radius of a circle centered in the center of the grid. The corresponding values on the y -axis represent the successful grasp percentage for each sphere when the object to-be-grasped is placed within that circle. Each plot compares the performance obtained with the rigid Delta and the SoftHandler. (a) Results of the small light sphere. (b) Results of the medium light sphere. (c) Results of the big light sphere. (d) Average of the results obtained with the light spheres. (e) Results of the small heavy sphere. (f) Results of the medium heavy sphere. (g) Results of the big heavy sphere. (h) Average of the results obtained with the heavy spheres. (i) Average of the results obtained for the small spheres. (j) Average of the results obtained with the medium spheres. (k) Average of the results obtained with the big spheres. (l) Average of the results obtained with all the spheres.

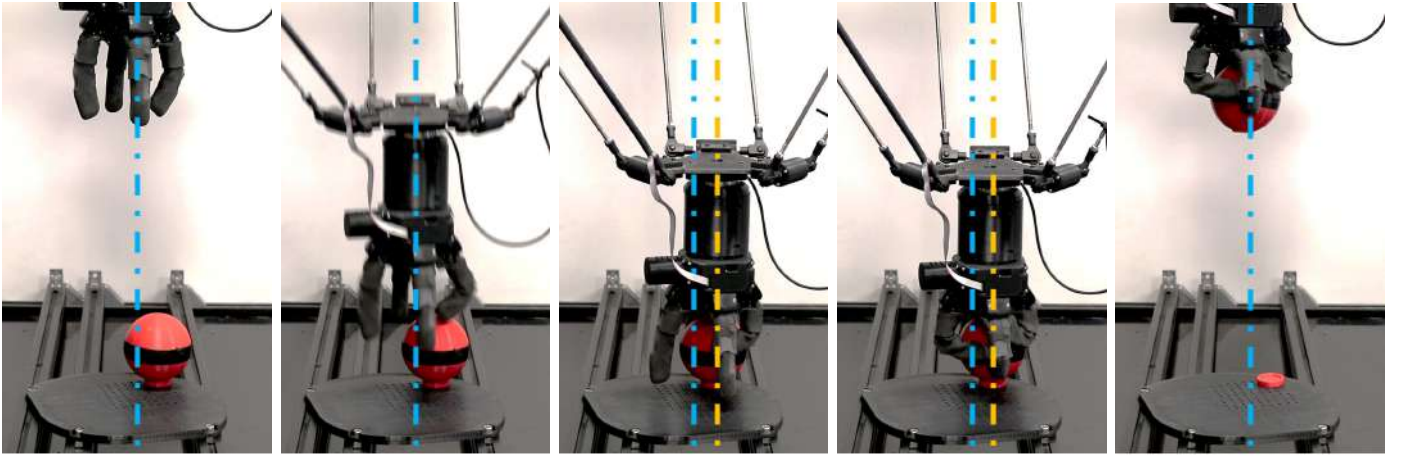
placement increases. This obvious result is due to the fact that larger displacements lead to grasps that do not follow the caging primitive, i.e. weaker grasps. An example is an object grasped with only two fingers. In this case, heavier objects lead to easier slippage out of the end-effector. Given this observation, an actuation mechanism that leads to an adaptive end-effector position is momentous for grasping performance of the whole system. This result is shown in Fig. 9. This photo-sequence compares the performance of the SoftHandler with the one of the Rigid Delta. While approaching the big heavy sphere placed ~ 43 mm afar from the platform center, the Rigid Delta is not able to adapt the position of its end-effector due to the stiffness of its motion. On the other hand, the proposed device is able to passively adapt the position of its end-effector, moving it in the direction of the sphere, and it is able to grasp it. The vertical orange line highlights how much the gripper moved from the vertical blue line, i.e. the reference position (please refer to the video footage for more details).

This result is intuitive for big heavy objects, nevertheless it is also present for lighter objects, although attenuated. Indeed, two effects arise. First, if the object is particularly lightweight, also a minor force due to the interaction with a stiff system could be sufficient to move it from the grasping volume of the gripper. On the other hand, if the device has a compliant behavior, the force peak can be filtered. The second reason is due to the small size of the object. Fig. 8(i) shows that the worsening effect due to the displacement increases in the case of smaller objects. This is caused by the fact that, given a large displacement, there is no contact between the gripper fingers and the small sphere. In particular, in this experiment the small sphere is completely out of the grasping volume of the gripper in the case of the largest displacement.

The grasping success rate is a parameter of paramount importance because it affects the speed performance of the manipulator. Indeed, if the time required to complete one grasping cycle is T , the total task time to execute a series of



(a) Rigid Delta.



(b) SoftHandler.

Fig. 9. Photo-sequence of the Delta grasping the big heavy sphere in presence of a displacement of ~ 43 mm. (a) the Rigid Delta fails to grasp the object, notwithstanding it is equipped with the SoftGripper. (b) The intrinsic adaptivity of the SoftDelta permits to readjust the end-effector position, moving it from the vertical blue line to the vertical orange line.

n cycles (e.g. to empty a basket of n oranges) has an expected value of $T_{\text{tot}} = \frac{n}{\gamma} T$, where γ is the grasping success rate. A direct consequence of this is that, for a rigid manipulator, to be as fast as the SoftHandler, should feature a faster cycling time

$$T_R < \frac{\gamma_R}{\gamma_S} T_S, \quad (6)$$

where γ_S and γ_R are the probability of obtaining a successful grasp with the SoftHandler and the rigid Delta, respectively, while T_S and T_R are the cycling time of the SoftHandler and the rigid Delta, respectively. This means that, assuming e.g. a maximum displacement error of 30mm we get (from Fig. 8(1)) $\gamma_S = 0.983$ and $\gamma_R = 0.713$, thus the rigid robot should be 38% faster to recover the loss of performance due to the larger failure rate.

Finally, Fig. 7 compares the forces applied by the rigid robot with the forces applied by the SoftHandler. In the case of the small spheres, the forces are comparable for both devices. This is due to the scarcity of interactions since the

objects are small and the grasping approach is tuned on the biggest object. Notwithstanding the comparable forces, the SoftHandler performance remains better in terms of grasping success rate. Instead, in the cases of medium and big spheres the forces applied by the rigid robot during the grasping phase are larger since interactions between the object and the SoftGripper are major.

B. Force at the End-Effector

In this section we analyze the results obtained with the SoftDelta, comparing the experimental force measurements with the force estimated with the Cartesian stiffness model. Given (1), (2), a configuration of the SoftDelta \mathbf{q} and the wrench due to the end-effector weight, it is possible to compute the Cartesian stiffness through (4). We choose $q_i = -0.2443\text{rad}$, $i = 1, \dots, 3$, i.e. the configuration corresponding to the grasping phase. Given K_C , we can estimate the applied force \mathbf{f} as

$$\tilde{\mathbf{f}} = K_C \cdot \Delta \mathbf{x}, \quad (7)$$

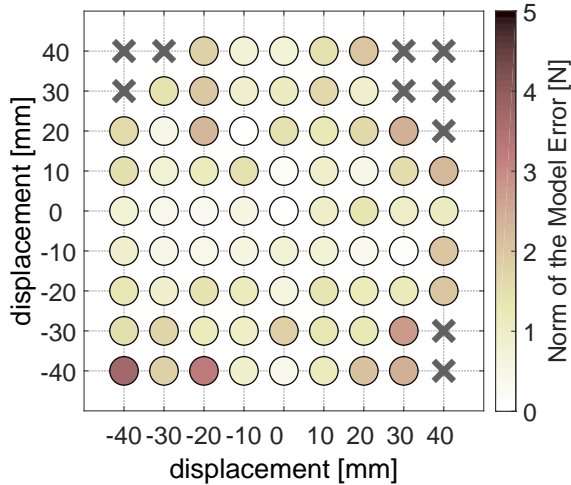


Fig. 10. Comparison between the experimental and the estimated force. A cross marker means that the SoftHandler failed to grasp all the spheres given that displacement, while a circle represents a success. The color-map of the circles represents the metric (10).

where $\Delta \mathbf{x}$ is the Cartesian displacement from the reference position. Considering the grasping phase as reference, the vector of the Cartesian displacement $\Delta \mathbf{x}_n$ for each node n ($n = 1 \dots 81$) of the grid is equal, in the XY plane, to the grid displacement itself (Fig. 6(a)). Given this observation, we obtain the estimate of the applied force $\tilde{\mathbf{f}}_n = [\tilde{f}_{x,n}, \tilde{f}_{y,n}, \tilde{f}_{z,n}]^T$ for each nodal displacement n ($n = 1 \dots 81$). Note that, since there is no a-priori information about the displacement along the z-axis, we will assume it equal to zero, and we will omit the force measurement $\tilde{f}_{z,n}$ in the next analysis.

Given the experimental force measurements $\mathbf{f}_{s,n}(t) = [f_{x,s,n}(t), f_{y,s,n}(t), f_{z,s,n}(t)]^T$, where t is the time variable, s is the sphere index ($s = 1 \dots 6$), and n ($n = 1 \dots 81$) is the nodal position on the grid, we define the force vector $\mathbf{f}_{s,n}^* = [f_{x,s,n}^*, f_{y,s,n}^*, f_{z,s,n}^*]^T$ corresponding to the peak value of force norm during the grasping approach as

$$\mathbf{f}_{s,n}^* \triangleq \mathbf{f}_{s,n}(t_{s,n}^*) = \begin{bmatrix} f_{x,s,n}(t_{s,n}^*) \\ f_{y,s,n}(t_{s,n}^*) \\ f_{z,s,n}(t_{s,n}^*) \end{bmatrix}, \forall s = 1 \dots 6, n = 1 \dots 81, \quad (8)$$

where $t_{s,n}^* = \arg \max_t (|\mathbf{f}_{s,n}(t)|)$. Given (8), we then average the results of the successful grasps among the six spheres. Thus, we define the vector of the average measured force as

$$\bar{\mathbf{f}}_n \triangleq \frac{1}{N_n} \sum_{s \in \mathcal{S}_n} \mathbf{f}_{s,n}^*, \forall n = 1 \dots 81, \quad (9)$$

where \mathcal{S}_n is the set containing the indexes of the spheres successfully grasped at the n -th displacement, and N_n is the cardinality of \mathcal{S}_n . Given (9) we introduce the performance metric related to the n -th grid displacement. We define it as the norm of the error between the force vector estimated from the Cartesian stiffness model and the force measurements

$$P_n \triangleq \left\| \begin{bmatrix} \tilde{f}_{x,n} - \bar{f}_{x,n} \\ \tilde{f}_{y,n} - \bar{f}_{y,n} \end{bmatrix} \right\|, \forall n = 1 \dots 81. \quad (10)$$

Fig. 10 reports the comparison between the experimental force measurements and the estimated force measurements. A cross marker means that the SoftHandler failed to grasp all the spheres given that displacement, while a circle represents a success. The color-map of the circles represents the value of the metric (10). The error between the two values has a mean value of 1.24N and a peak value of 3.74N corresponding to a displacement of 57mm. The difference between the model and the experimental results increases with the displacement.

V. SYSTEM VALIDATION

In this section we show the robot effectiveness in various grasping tasks where several heterogeneous objects are involved. Several experimental results on the applications discussed in Sec. II are presented, with the final goal of testing the SoftHandler in realistic scenarios. The selected tasks consist in the picking and placing objects from a crate to another one. The objective is to empty the picking crate. As a preliminary validation, we show the SoftHandler grasping a series of objects with a wide variety of physical and geometrical properties. Then, we test the behavior of the robot when the picking crate contains several objects, simulating two different scenarios (raw food handling and bin picking) with two different object configurations. Thus, we show first how the SoftHandler compliance allows to grasp objects that present a broad variety of physical properties. Then, we test the ability of the robot in picking items from a cluttered crate.

1) *Experimental Setup*: Two $600 \times 400 \times 100$ mm crates are placed under the SoftHandler, one with the objects to-be-picked and one empty where the objects have to be placed. An Asus Xtion-Pro camera is mounted on the robot frame. This RGB-D camera is used to sense the XYZ position of the objects to be picked. The vision system implements the Euclidean Cluster Extraction (ECE) algorithm. This segmentation method is used to sense XYZ position of the cluster (the Z element is chosen as the highest one for each cluster). Fig. 11 illustrates the vision system operating principle. The real scene (11(a)) is perceived by the camera that senses the point cloud (11(b)). The point cloud is divided into clusters and a frame is assigned to each cluster (11(c)). Note that some clusters may include more than one object. Finally, the vision system chooses which object is the next to be picked and sends the position to the control system. Note that only the position of the respective frame is passed to the control system, with no information about the cluster.

Given the randomness of the object locations, the ILC control architecture described in Sec. III-C can not be applied, unless limiting the object positions to a few known fixed points. Since our goal is to test the proposed system in a realistic scenario, we prefer to adopt the PID approach instead. The stiffness configuration of the SoftHandler is set to the minimum in order to preserve the integrity of these fragile objects. As described in Sec. III-C, the effects of employing an inverse kinematics with a low-tuned PID control instead of the ILC approach are twofold. First, there is a stiffening of the robot joint caused by the feedback term

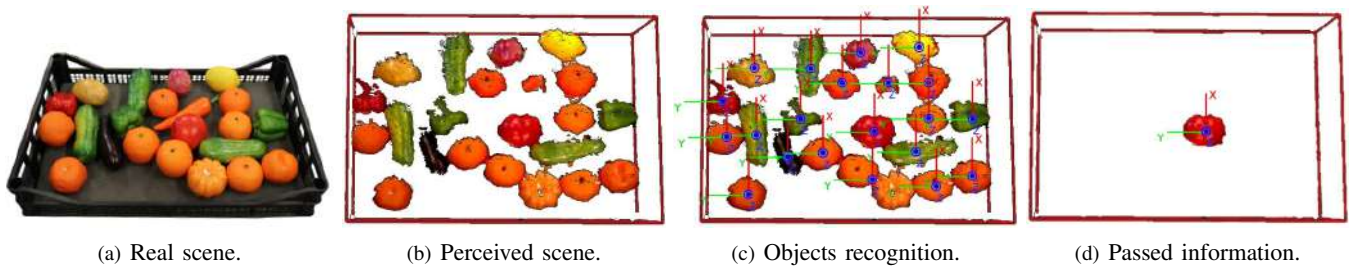


Fig. 11. Pipeline of the vision system. The real scene (a) is perceived by an RGB-D camera that senses the point cloud (b). The point cloud is divided into clusters and a frame is assigned to each cluster (c). The vision system sends to the control system only the frame linked to one cluster (d).

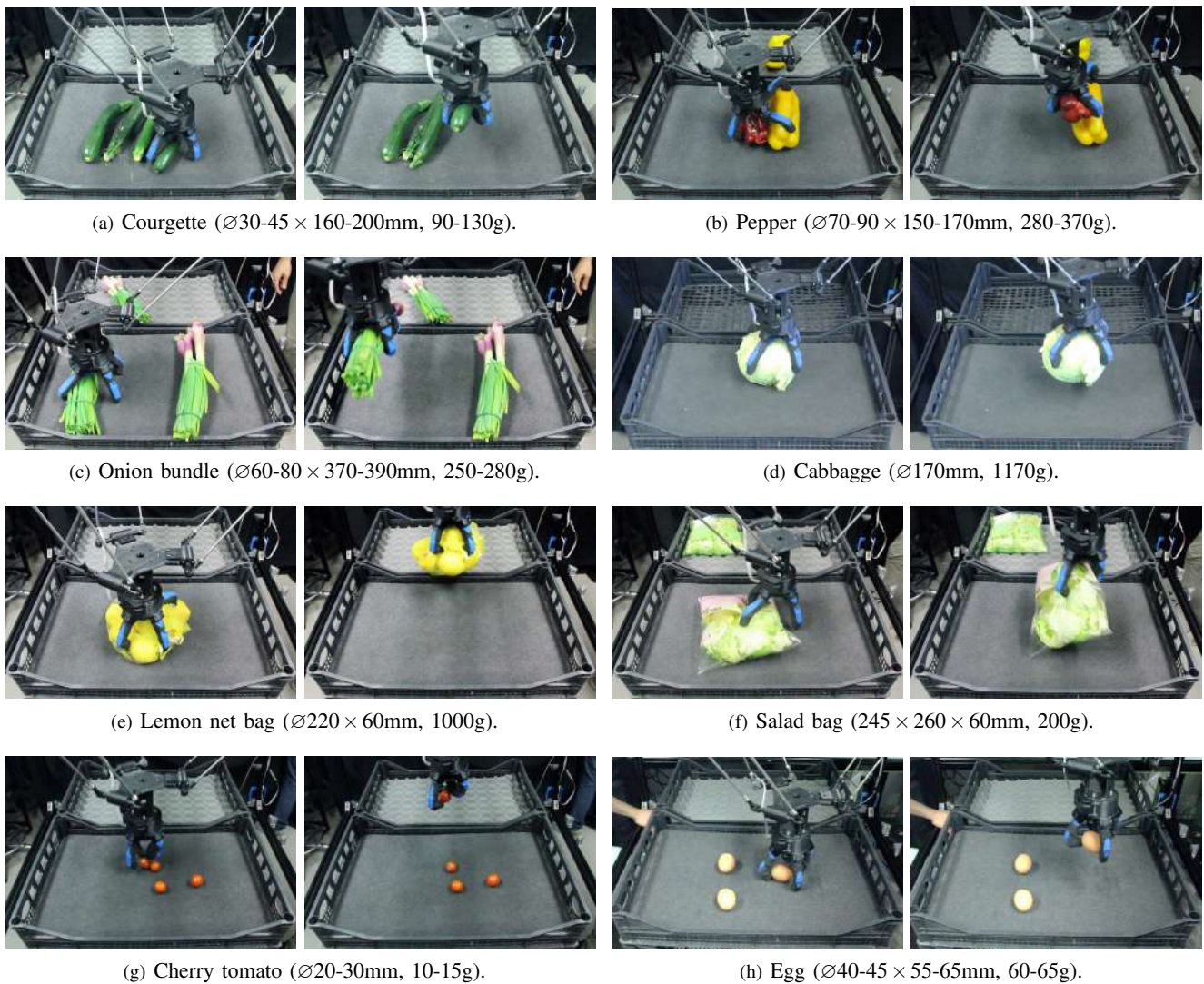


Fig. 12. Raw vegetables and fruits handling photo-sequences. The SoftHandler is able to grasp objects with several different size, shape, weight, texture and stiffness. Note that, given the irregularity of the shape of involved objects, the reported dimensions are an approximation of the real ones.

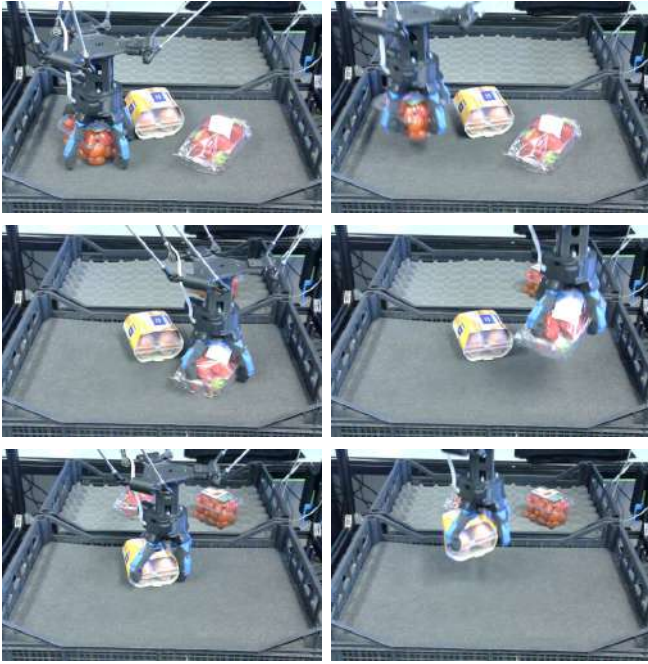


Fig. 13. Grocery handling scenario: tomato package ($185 \times 120 \times 110\text{mm}$, 500g), strawberry package ($185 \times 115 \times 90\text{mm}$, 500g), and egg package ($155 \times 110 \times 80\text{mm}$, 420g).

in the control law. Since the chosen gains of the PID are low, the theoretical maximum stiffness variation is equal to $0.0166 \frac{\text{Nm}}{\text{rad}}$. The second effect is the worsening of the tracking performance. Indeed, the root mean square of the tracking error (averaged between the trials presented in the following) is more than doubled than the one obtained in the experiment in Sec. IV-A, resulting in a mean positioning error of the end-effector equal to 23.58mm. While the first issue can not be solved unless adopting a different control law, the second issue appears to be less crucial given the system characterization in Sec. IV-A. Indeed, from Fig. 8(l) we expect a success rate of about 99% for a displacement equal to 23.58mm.

2) *Experiments*: Three sets of experiments are presented.

Preliminary Validation: As described in Sec. II, handling of raw food and groceries involve unorganized objects with a wide variety of sizes, shapes, weights, stiffnesses, textures and orientations. In Fig. 12 are depicted objects linked to a food handling task, while in Fig. 13 are depicted objects linked to a grocery handling task. Size and weight of each object are reported in the caption of the figures.

Validation in Raw Food Handling Scenario: In the first two experiments, the objects involved in the task are apples, thus they present homogeneous geometrical characteristics ($\varnothing 80\text{-}95\text{mm}$, 200-280g). Fig. 14(a) shows the setup of Experiment 1. Here the 10 objects are disorganized and can move freely in the crate. On the other hand, in Fig. 14(b) is depicted the second setup of the raw food handling scenario (Experiment 2). In this case, the 7 items are ordered and partially constrained. Indeed, the plastic fruit support

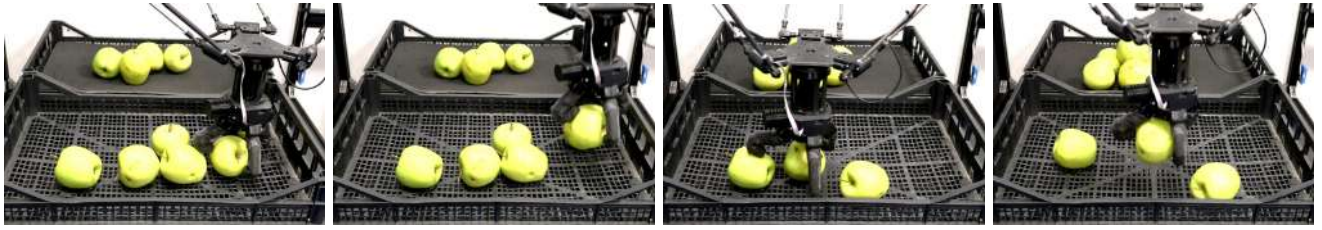
prevents any movement of the apples in the XY plane. In Experiment 3, the SoftHandler is tested in an challenging condition: grasping disorganized and heterogeneous objects. In this task the 30 employed objects are toy fruits with different shapes and sizes ($\varnothing 25\text{-}80 \times 50\text{-}170\text{mm}$, 8-20g). Fig. 15 shows the setup.

Validation in Bin Picking Scenario: Experiment 4 and 5 are related to the bin picking scenario. The objects to-be-picked are rubber gears. All the items present the same complex geometry and weight ($\varnothing 90 \times 130\text{mm}$, 180g). In the first scenario (Experiment 4, Fig. 16(a)), 7 gear covers are randomly placed in the crate and are free to move. In the second setup (Experiment 5, Fig. 16(b)), 6 gear covers are stacked into 3 columns of 2 elements each.

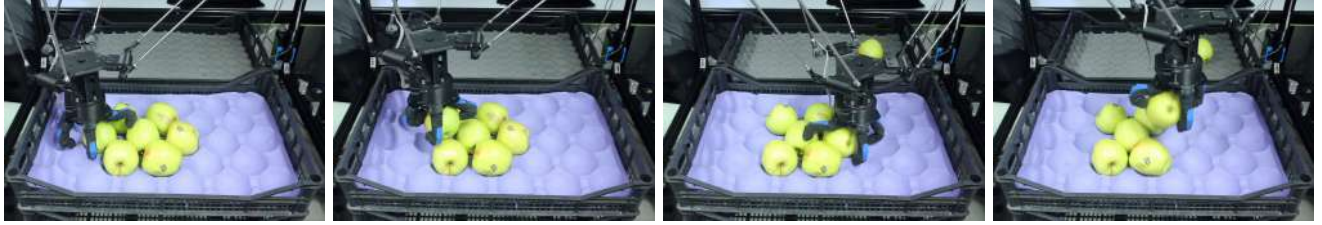
3) *Results*: In Experiment 1 all the apples are moved in approximately 120s. The grasping success rate is 83%, this means that each apple needs 1.2 cycles to be moved. In Experiment 2 all the apples are moved in $\sim 150\text{s}$. The grasping success rate is 78%, this means that each apple needs 1.3 cycles to be moved. In Experiment 3 the task is completed in $\sim 150\text{s}$. The grasping success rate is approximately 69%, that translates into 1.4 cycles for each item. In Experiment 4 all the objects are moved in $\sim 80\text{s}$. The grasping success rate is 87%, this means that each gear cover needs 1.1 cycles to be moved. In Experiment 5 all the items are moved in $\sim 110\text{s}$. The grasping success rate is 100%, this means that each gear cover needs 1 cycle to be moved.

4) *Discussion*: Several graspable objects are reported in Fig. 12 and in Fig. 13. Fig. 12(a) shows the SoftHandler grasping a courgette, while Fig. 12(b) shows how the proposed device adapts to the pepper shape. Fig. 12(c) shows the robot ability to grasp large objects like an onion bundle, while Fig. 12(d) shows how the SoftGripper fingers adapt to a large cabbage too. The robot is also able to grasp an heavy object (Fig. 12(d) and Fig. 12(e)). Note that the weight perceived by the manipulator and the shape of the object change during the grasp of the net bag full of lemons. Notwithstanding the ability of the SoftHandler to handle heavy payloads, Fig. 12(f-h) display how the compliance elements of the SoftHandler allows also to handle fragile objects. In Fig. 12(f) the robot grasps a delicate salad bag. In Fig. 12(g) it is shown how cherry tomatoes can be picked despite of their tiny size. Fig. 12(h) shows that the proposed device can handle also eggs. Finally, in Fig. 13 is depicted a grocery handling task. The proposed system grasps a cherry tomato, a strawberry and an egg package in sequence. It is worth noting that none of the objects presented any kind of damage at the end of the experiment.

In Experiment 1 (Fig. 14(a)) the apples are unorganized and can move freely in the XY plane. This allows an easier positioning of the gripper fingers in-between the objects, that leads to a full envelope of the object, hence to more stable grasps. At the same time, a moving object may cause measurement errors in the vision system. In Experiment 2 (Fig. 14(b)) the fruit support hinders the positioning of the fingers in-between the objects, but it enhances the adaptation of the end-effector. In Experiment 3 (Fig. 15) the



(a) Photo-sequence of Experiment 1: unordered apples task.



(b) Photo-sequence of Experiment 2: ordered apples task.

Fig. 14. Raw food handling scenario: emptying a crate of apples. The objects share homogeneous physical and geometrical characteristics, i.e. $\varnothing 80\text{-}95\text{mm}$, $200\text{-}280\text{g}$. Two scenarios are presented: (a) 10 apples are randomly placed and are free to move within the crate. (b) 7 apples are ordered and partially constrained by the plastic fruit support.

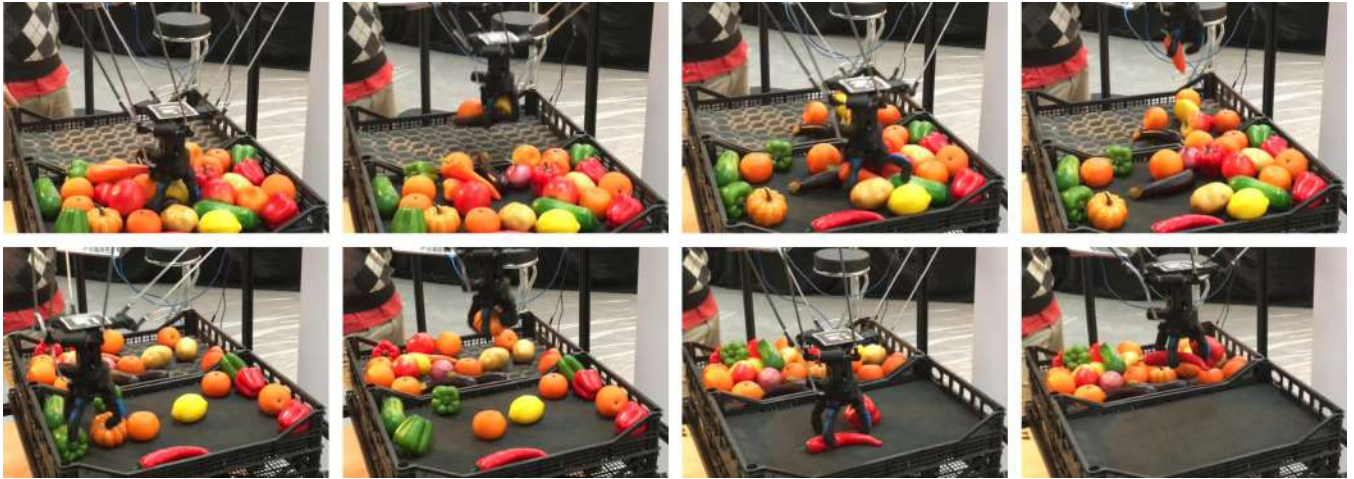


Fig. 15. Raw food handling scenario. Photo-sequence of Experiment 3. The SoftHandler empties a crate full of toy fruits. The objects differ in shape and size, and they are randomly placed within the crate. The size range of the objects is $\varnothing 25\text{-}80 \times 50\text{-}170\text{mm}$, while the weight range is $8\text{-}20\text{g}$

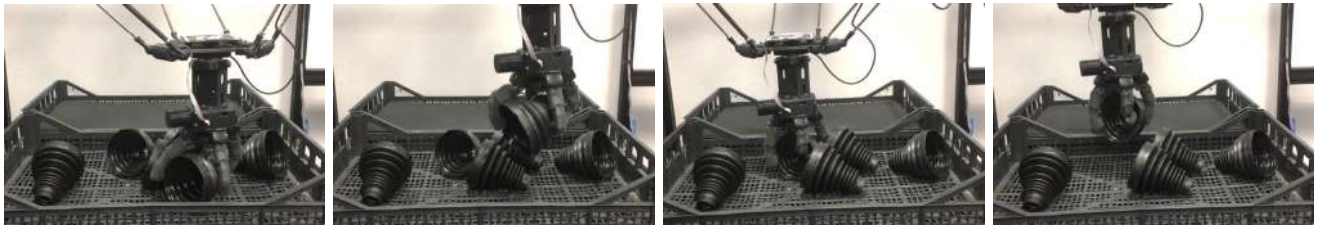
objects are disorganized, heterogeneous and cluttered. It is worth mentioning that the employed grasping approach is equal independently from the object geometrical properties. Finally, in Experiment 4 (Fig. 16(a)) the rubber gear covers are placed randomly in position and orientation, while in Experiment 5 (Fig. 16(b)) the objects are orderly stacked.

In all the experiments the proposed system is able to move the 100% of the objects, successfully completing the task. It is worth noting how the SoftGripper fingers behave differently also when grasping similar objects. This is linked to the position and orientation of the object as to potential constraints. Fig. 14 highlights this point. The apples are grasped with different finger configurations depending on how much the scene is cluttered. In Fig. 16(a), different orientations of the object lead to different gripper grasps. In

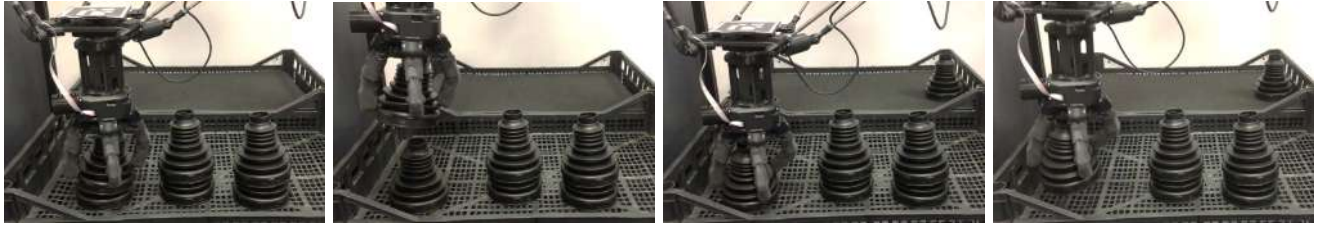
some cases, the object can be grasped also with a reduced number of fingers. This is the case of the carrot in Fig. 15 that is grasped with only two fingers instead of four. Finally, in the video attachment it is possible to notice that the SoftHandler end-effector adapts to the apple position.

VI. GENERAL DISCUSSION

Sec. IV showed a comparison between the SoftHandler and a comparable rigid manipulator, while Sec. V presented a validation of the system in grasping objects presenting a broad variety of physical and geometrical characteristics. During the experiments we observed that some of the grasp may fail during the execution of the task. Mostly observed unsuccessful grasps were due to two different types of failure: *slipping* and *missing*.



(a) Photo-sequence of Experiment 4: unordered rubber gear covers task.



(b) Photo-sequence of Experiment 5: ordered rubber gear covers task.

Fig. 16. Bin picking scenario: emptying a crate of rubber gear covers. The objects share homogeneous complex physical and geometrical characteristics, i.e. $\varnothing 90 \times 130\text{mm}$, 180g. Two scenarios are presented: (a) 7 gear covers are randomly placed and are free to move within the crate. (b) 6 objects are stacked into 3 columns of 2 elements each.

We refer to *slipping* when the grasped item slips out of the gripper fingers. This issue occurs, for example, in Experiment 3 (Fig. 15). The failure is linked to grasps where the fingers do not completely cage the object. This may happen when the displacement between the end-effector and the object is large. As suggested by Fig. 8(i) and 8(h), tiny objects and heavy objects are the most challenging ones, especially when the displacement is large. Another reason for *slipping* can be a wrong grasping approach. Indeed, in all the experiments we employed the same grasping approach without any specific tuning on the item to-be-picked. Future works will analyze different grasping approaches for different object geometries.

On the other hand, we refer to *missing* when the end-effector is placed where there are no objects. This issue is related to the vision system that passes a wrong position of the fruit to-be-picked to the control system. If we ignore this type of fault, the success rate increases from 83% to 100% (Experiment 1 - Fig. 14(a)), from 78% to 100% (Experiment 2 - Fig. 14(b)), from 69% to 81% (Experiment 3 - Fig. 15) and from 87% to 100% (Experiment 4 - Fig. 16(a)), respectively. During Experiment 5 (Fig. 16(b)) no vision errors occurred. Thus, the average grasping success rate neglecting the vision errors is 96%. Interestingly, this result is close to the success rate obtained in Sec. IV-A. Indeed, the average positioning error of the end-effector during Experiments 1-5 is 23.58mm, which corresponds to a success rate of 99%, according to Fig. 8(l). The difference between the two values can be ascribed to experimental variability and differences in the setup, which include different controllers and different manipulated objects.

Another issue to consider is the *double-grasp*, i.e. when the gripper closes around more than one object. This tends to occur when the objects are cluttered (e.g. Fig. 15), and the adopted vision system merges close items into one cluster. A *double-grasp* may resolve in either no picking, picking a

single item or picking more than one. Each of these result could be considered a failure or not depending on the task. Employing a different grasping approach or a different vision system may solve this behavior.

The quantitative experiments in Sec. V let us appraise the average picking time of the SoftHandler, which amounts to $\sim 10\text{s}$. The most important factor limiting the speed of the system is the power of the adopted actuators, which are mainly intended for research purposes. Indeed, Fig. 4(d) shows that their maximum velocity is lower than the one of most industrial manipulators. On the other hand, our goal was not to develop a system highly optimized in terms of speed performance, rather to explore the development of a device for handling of heterogeneous and fragile objects, that is robust to accidental impacts. Future works will aim to improve the actuation performance and, more in general, the system performance.

A second factor limiting the speed of the system is linked to the vision system. Each failure in the vision system leads to an additional cycle to empty the crate, resulting in longer task completion time. Experiments in Sec. V showed that the employed vision system presents an average failing rate equal to 15%.

Nevertheless, the type of task plays an important role in evaluating the speed of the system. Usually, the tasks where the robot achieves the fastest performance are those where the objects are small, ordered and perfectly known. Here, we are tackling a completely different task, i.e. picking and placing of heterogeneous unknown objects. As suggested by the results in Sec. IV, in the case under analysis, rigid manipulators exhibit lower grasping performance (i.e. more failures), influencing the total task completion time.

However, in presence of a displacement error, the SoftHandler can grasp a wide variety of objects with a performance superior to a comparable rigid robot, both in terms

of grasping success rate and applied contact forces. The former metric leads to a better efficiency in terms of total task completion time. Instead, lower applied contact forces increase the object integrity preservation and also the device robustness.

VII. CONCLUSIONS

In this work, we tackled the challenge of industrial pick-and-place tasks, presenting a novel robotic system based on soft robotic technologies. The developed system, namely SoftHandler, integrates a variable stiffness delta manipulator (SoftDelta) and a soft articulated gripper (Pisa/IIT SoftGripper) in order to overcome limitations of traditional rigid robots. We presented the system mechanical design and control architecture, and we analyzed its Cartesian stiffness.

We designed a benchmarking method to compare the proposed device with a rigid manipulator with an equal kinematic structure, same soft end-effector and analogous actuation performance. This paper is one of the few that presents a direct juxtaposition of a multi-joint compliant robot and its conventional and rigid counterpart. Results show that the SoftHandler achieves a higher grasping success rate in presence of positioning or measurement errors, resulting in a more robust behavior. Furthermore, results show also that the rigid robot presents larger applied forces in the grasping phase, resulting in a potentially harmful behavior both for human beings, grasped objects and the robot itself.

Finally, the effectiveness of the SoftHandler was tested in realistic scenarios. First, we performed various grasping tests on a set of real objects presenting different geometries and organizations. Then, we tested the performance of the systems in a handling task of raw food and industrial parts. Results show that the compliant elements of the proposed device allow to grasp a wide variety of real objects in different scenario while preserving their integrity.

ACKNOWLEDGMENT

This research has received funding from the European Union's Horizon 2020 Research and Innovation Programme under Grant Agreement No. 645599 (Soma) and No. 840446 (SoftHandler). The content of this publication is the sole responsibility of the authors. The European Commission or its services cannot be held responsible for any use that may be made of the information it contains. The authors would like to thank Riccardo Persichini and Alessandro Raugi from qrobotics, and Mattia Poggiani from Istituto Italiano di Tecnologia.

REFERENCES

- [1] Daniela Rus and Michael T Tolley. Design, fabrication and control of soft robots. *Nature*, 521(7553):467, 2015.
- [2] Cosimo Della Santina, Cristina Piazza, Gian Maria Gasparri, Manuel Bonilla, Manuel Giuseppe Catalano, Giorgio Grioli, Manolo Garabini, and Antonio Bicchi. The quest for natural machine motion: An open platform to fast-prototyping articulated soft robots. *IEEE Robotics & Automation Magazine*, 24(1):48–56, 2017.
- [3] Raphael Deimel and Oliver Brock. A novel type of compliant and underactuated robotic hand for dexterous grasping. *The International Journal of Robotics Research*, 35(1-3):161–185, 2016.

- [4] Manuel Bonilla, Edoardo Farnioli, Cristina Piazza, M Catalano, Giorgio Grioli, Manolo Garabini, Marco Gabiccini, and Antonio Bicchi. Grasping with soft hands. In *Humanoid Robots (Humanoids), 2014 14th IEEE-RAS International Conference on*, pages 581–587. IEEE, 2014.
- [5] Francesca Negrello, Manolo Garabini, Giorgio Grioli, Nikolaos Tsagarakis, Antonio Bicchi, and Manuel G. Catalano. Benchmarking resilience of artificial hands. In *Robotics and Automation (ICRA), 2019 IEEE International Conference on*. IEEE, 2019.
- [6] Clemens Eppner, Raphael Deimel, José Alvarez-Ruiz, Marianne Maertens, and Oliver Brock. Exploitation of environmental constraints in human and robotic grasping. *The International Journal of Robotics Research*, 34(7):1021–1038, 2015.
- [7] Steffen Puhlmann, Fabian Heinemann, Oliver Brock, and Marianne Maertens. A compact representation of human single-object grasping. In *Intelligent Robots and Systems (IROS), 2016 IEEE/RSJ International Conference on*, pages 1954–1959. IEEE, 2016.
- [8] J Brinker and B Corves. A survey on parallel robots with delta-like architecture. In *Proceedings of the 14th IFToMM World Congress*, pages 407–414, 2015.
- [9] Bram Vanderborght, Alin Albu-Schäffer, Antonio Bicchi, Etienne Burdet, Darwin G Caldwell, Raffaella Carloni, M Catalano, Oliver Eiberger, Werner Friedl, Ganesh Ganesh, et al. Variable impedance actuators: A review. *Robotics and Autonomous Systems*, 61(12):1601–1614, 2013.
- [10] Franco Angelini, Cosimo Della Santina, Manolo Garabini, Matteo Bianchi, Gian Maria Gasparri, Giorgio Grioli, Manuel Giuseppe Catalano, and Antonio Bicchi. Decentralized trajectory tracking control for soft robots interacting with the environment. *IEEE Transactions on Robotics*, 2018.
- [11] Aaron M Dollar and Robert D Howe. Towards grasping in unstructured environments: Grasper compliance and configuration optimization. *Advanced Robotics*, 19(5):523–543, 2005.
- [12] Eric Brown, Nicholas Rodenberg, John Amend, Annan Mozeika, Erik Steltz, Mitchell R Zakin, Hod Lipson, and Heinrich M Jaeger. Universal robotic gripper based on the jamming of granular material. *Proceedings of the National Academy of Sciences*, 107(44):18809–18814, 2010.
- [13] Paul Glick, Srinivasan Suresh, Donald Ruffatto III, Mark Cutkosky, Michael T Tolley, and Aaron Parness. A soft robotic gripper with gecko-inspired adhesive. *IEEE Robotics and Automation Letters*, 2018.
- [14] Robotiq. Robotiq adaptive gripper: Specification sheet. Available at: <https://robotiq.com/products/3-finger-adaptive-robot-gripper>.
- [15] Lael U Odhner, Leif P Jentoft, Mark R Claffee, Nicholas Corson, Yaroslav Tenzer, Raymond R Ma, Martin Buehler, Robert Kohout, Robert D Howe, and Aaron M Dollar. A compliant, underactuated hand for robust manipulation. *The International Journal of Robotics Research*, 33(5):736–752, 2014.
- [16] Raymond R Ma, Lael U Odhner, and Aaron M Dollar. A modular, open-source 3d printed underactuated hand. In *Robotics and Automation (ICRA), 2013 IEEE International Conference on*, pages 2737–2743. IEEE, 2013.
- [17] Domenico Mura, Manuel Barbarossa, Giacomo Dinuzzi, Giorgio Grioli, Andrea Caiti, and Manuel G Catalano. A soft modular end effector for underwater manipulation: A gentle, adaptable grasp for the ocean depths. *IEEE Robotics & Automation Magazine*, 25(4):45–56, 2018.
- [18] TK Lien. Gripper technologies for food industry robots. In *Robotics and Automation in the Food Industry*, pages 143–170. Elsevier, 2013.
- [19] Gualtiero Fantoni, Marco Santochi, Gino Dini, Kirsten Tracht, Bernd Scholz-Reiter, Juergen Fleischer, Terje Kristoffer Lien, Guenther Seliger, Gunther Reinhart, Joerg Franke, et al. Grasping devices and methods in automated production processes. *CIRP Annals-Manufacturing Technology*, 63(2):679–701, 2014.
- [20] R Morales, FJ Badesa, N Garcia-Aracil, JM Sabater, and L Zollo. Soft robotic manipulation of onions and artichokes in the food industry. *Advances in Mechanical Engineering*, 6:345291, 2014.
- [21] A Albu-Schaffer, Max Fischer, Günter Schreiber, Florian Schoeppe, and Gerd Hirzinger. Soft robotics: what cartesian stiffness can obtain with passively compliant, uncoupled joints? In *2004 IEEE/RSJ International Conference on Intelligent Robots and Systems (IROS)(IEEE Cat. No. 04CH37566)*, volume 4, pages 3295–3301. IEEE, 2004.
- [22] Lung-Wen Tsai. *Robot analysis: the mechanics of serial and parallel manipulators*. John Wiley & Sons, 1999.
- [23] Florian Petit, Andreas Daasch, and Alin Albu-Schäffer. Backstepping

control of variable stiffness robots. *IEEE Transactions on Control Systems Technology*, 23(6):2195–2202, 2015.

- [24] Gabriele Buondonno and Alessandro De Luca. Efficient computation of inverse dynamics and feedback linearization for vsa-based robots. *IEEE robotics and automation letters*, 1(2):908–915, 2016.